CHAPTER 5: DESIGN OPTIMISATION OF SEN

All preceding work described in this dissertation constitute the stepping-stones towards the ultimate design optimisation of the SEN.

Design optimisation in the current field of application involves a few disciplines, woven into one composite process:

- CFD analysis
- Fluid mechanics (intervention of user required as explained in Literature Survey)
- Experimental Analysis
- Mathematical Optimisation
    - Engineering insight to:
        - identify candidate objective functions and constraint functions to ultimately obtain an "optimum" SEN design
        - identify all parameters, and select optimisation variables from these parameters to meaningfully express the objective and constraint functions
    - Classical formulation of optimisation problem [53]
    - Selection of optimisation algorithm
- Automation procedures of all of the above

Firstly, the automation procedures used in this dissertation will be expounded on, followed by formulating the classical design optimisation problem. Finally, the entire optimisation process will be illustrated using an example of a 2D SEN design optimisation exercise. Finally, due to computational limitations, an initial 3D SEN design space exploration will be conducted.

5.1 Automation of Optimisation process

As a meaningful design optimisation exercise may require at least three (3) design iterations (each consisting of a number of perturbations, depending on the number of design variables), it is crucial that the design optimisation process is automated.

5.1.1 Parameterisation: Automation of grid generation

The first step in any CFD model is the creation of geometry, and the discretisation of this geometry into cells (small volumes (3D) or areas (2D)), which is called meshing.

With design optimisation, it is desirable to create meshed geometries by just specifying a pre-programmed parameter. This idea (called parameterisation) will be described using a 2D SEN as an example.

Figure 5.1 shows a 2D SEN design with a number of possible parameters. Only 4 of these parameters were chosen as design variables:

- x_1 = SEN port angle
- x_2 = SEN port height
- x_3 = well depth
- x_4 = submergence depth

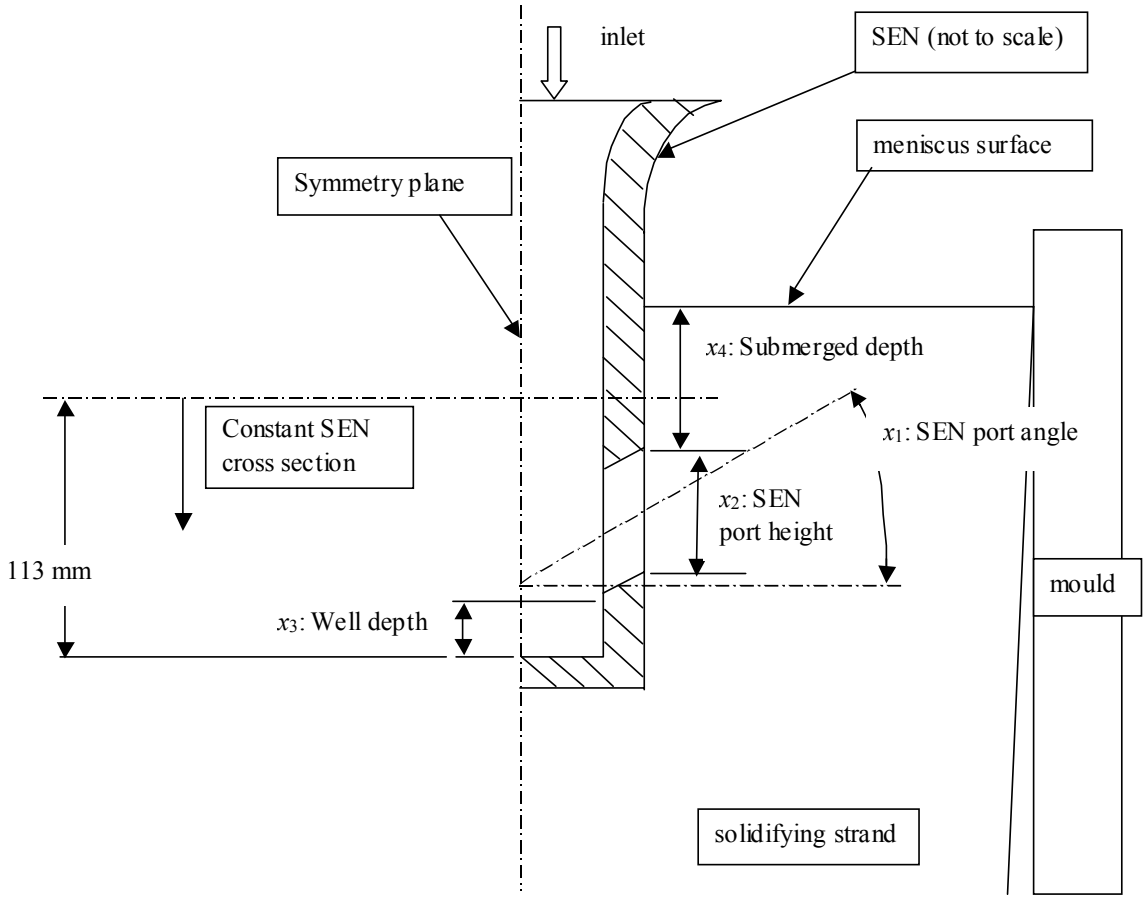

Figure 5.1: Design optimisation: parameterisation of 2D SEN

Suppose the base SEN design is similar to that of the new SEN of Columbus Steel with the base values for x_1, x_2, x_3, x_4 or $\boldsymbol{x}^{(1,0)}$. The superscript (1,0) indicates the base case (0) of the first design iteration (1).[1]

Scripting capability

The pre-processor, GAMBIT [11], has a scripting capability that enables a user to parameterise a geometry and mesh. Instead of using the GUI (Graphical User Interface) of GAMBIT, the user can enter command lines one at a time, or a number of commands using a text file (~.txt). This text file is commonly known as the script file, and the pre-processor simply interprets these commands consecutively and sequentially.

It is thus conceivable that with the generation of the 2D SEN geometry in Figure 5.1, the specific angle of the SEN port (for example) is specified during the

[1] Another explanatory example: The second (2nd) perturbation of the third (3rd) design iteration would be expressed as $\boldsymbol{x}^{(3,2)} = [x_1 \ x_2 \ x_3 \ x_4]^{(3,2)}$

rendering process. GAMBIT enables the user to use a variable in such a case. For example: Instead of specifying the command:[2]

"`create vertex from vertex (0,0) at distance 20mm at angle 15`°"

the following command is given:

"`create vertex from vertex (0,0) at distance 20mm at angle %x1`"

The variable %x1 (thus x_1) can now be specified in the beginning of the script file, e.g.

"`%x1 = 15`".

Extrapolating this idea to the other variables, the geometry is considered to be parameterised. Consequently the following scenario is achievable:
By only specifying the variables %x1 (thus x_1), %x2, %x3 and %x4 at the beginning of the script file, the pre-processor will "automatically" render the geometry according to these specified parameters.

As briefly explained in the Literary Survey, the Optimiser suggests certain perturbations of the design (*i.e.*, other values for x_1, x_2, x_3, x_4) during each design iteration. It is however possible to automatically update the values in the script files using the optimiser LS-OPT. This fact already hints in a direction of total automatic optimisation. However, the entire automatic linking process (that also involves the CFD code) will be discussed in sections 5.1.2 and 5.4.

Apart from rendering the geometry (according to the specified or suggested design parameters) and meshing the geometry, the boundary types must be specified and named in the pre-processor GAMBIT to ensure correct interpretation by the CFD code FLUENT [10].

To summarise: in GAMBIT, all the necessary GUI inputs required for a meshed geometry can also be performed using a parameterised script file (or journal file), which can be edited automatically by the Optimiser.

[2] Note: Pseudo code is used here only to illustrate a point. The correct scripting code can be viewed in Appendix J.

For an example of such a script file, refer to Appendix J. This script file generates a 2D SEN geometry and mesh, similar to that in Figure 5.1.

5.1.2 Automation of CFD code - Optimiser interface

As explained in detail in Chapter 4, the geometry and mesh imported from GAMBIT, needs to be defined and configured before the CFD solution can be initialised. All the definitions and configurations for any CFD model are performed using the GUI of FLUENT.

FLUENT has the same scripting capability as GAMBIT (explained above in section 5.1.1): script commands are interpreted sequentially and consecutively from these text files by FLUENT. As the geometry changes during the design optimisation, the boundary types remain the same; subsequently the FLUENT script files remain unchanged in essence during an optimisation exercise. However, if a flow parameter is included in the optimisation as a design variable, the FLUENT script file would change.

There are two script files applicable to a CFD model evaluation in FLUENT:

- Set-up script file (as explained above)
- Run (monitoring data etc.) or convergence procedure script file

The run script file ensures that the solution procedure, as developed in Chapter 4 by trial and error methods, is followed with each CFD evaluation, to ensure repeatable convergence of each model and accompanying physical correctness.

Optimiser as interface and coordinator

The CFD code "package" (GAMBIT and FLUENT) cannot perform optimisation without an optimising code (henceforth referred to as the Optimiser).

The Optimiser, using the classically formulated optimisation problem, and starting from a base case design, uses the CFD code package to ultimately find an optimum design (set of optimised variables) that satisfies the original optimisation problem.

LS-OPT, the optimiser used in this dissertation, can be viewed as being mainly an optimisation algorithm, but with coordinating (scheduling) and interfacing capabilities.

The tasks of LS-OPT during a design iteration are best described in the company of a diagram. Refer to Figure 5.2 for the diagram that depicts the coordinating tasks performed during each iteration.

Description (to be read in conjunction with the diagram in Figure 5.2):
The heart of LS-OPT can be described as the optimisation algorithm that endeavours to minimise the objective function $f(\boldsymbol{x})$, satisfying the constraints $g(\boldsymbol{x})$ and $h(\boldsymbol{x})$.

Starting from a base case design, $\boldsymbol{x}^{(1,0)} = [x_1 \quad x_2 \quad x_3 \quad \ldots \quad x_n]$, LS-OPT needs to evaluate the base case (*i.e.*, run a CFD model and extract the relevant information) to

- establish the value of the objective function;
- establish whether the constraints are violated, or in what degree they are violated.

Firstly, LS-OPT updates the GAMBIT parameterised script file to contain the base case design $\boldsymbol{x}^{(1,0)}$, and execute GAMBIT with this script file as input. The GAMBIT output file is imported into FLUENT, simultaneously running the set-up script file. The desired geometry is now set up in FLUENT; consequently the run script file is executed. As soon as the CFD solution is converged, LS-OPT uses a similar script file to extract flow field data from the CFD solution (data was written to text files during solution convergence – as specified by the run script file). The data extracted from the converged solutions are also called responses. A

response can be a combination of information extracted from the converged CFD solution that LS-OPT uses to evaluate the objective and constraint functions.

LS-OPT now uses the flow field data to calculate the values of $f(\boldsymbol{x}^{(1,0)})$, $g(\boldsymbol{x}^{(1,0)})$ and $h(\boldsymbol{x}^{(1,0)})$.[3]
LS-OPT then chooses a first perturbation design ($\boldsymbol{x}^{(1,1)} = [x_1 \ x_2 \ x_3 \ \ldots \ x_n]$), with reference to the values calculated for the objective and constraint functions from the flow field data.

LS-OPT repeats the procedure described above for the first perturbation, until the required number of perturbations are evaluated. Suppose 8 perturbations are required by LS-OPT per design iteration: After evaluating perturbation design $\boldsymbol{x}^{(1,8)}$, LS-OPT uses its optimising algorithm to predict the optimum design $\boldsymbol{x}^{(1,*)}$ for the first design iteration, taking into account designs $\boldsymbol{x}^{(1,1)}$ to $\boldsymbol{x}^{(1,8)}$.

The optimum design of design iteration 1 ($\boldsymbol{x}^{(1,*)}$), doubles as the base case design for design iteration 2 ($\boldsymbol{x}^{(2,0)}$), and the entire process repeats itself until the optimisation problem has converged sufficiently.

[3] Traditionally in Mathematical Optimisation, *f(x)* refers to the objective function, *g(x)* to the inequality constraint function(s) and *h(x)* to the equality constraint function(s).

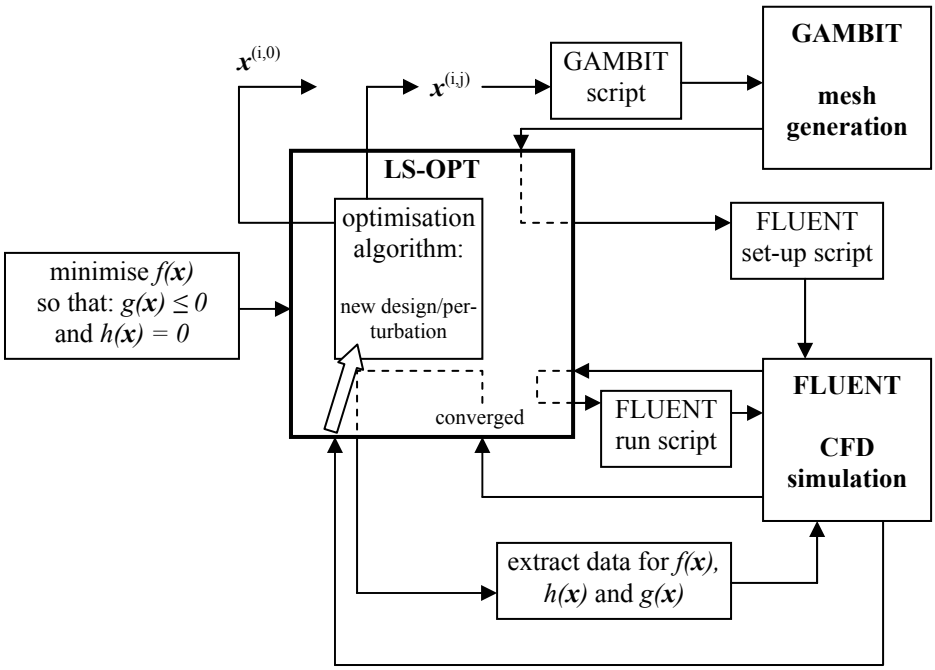

Figure 5.2: Diagram depicting the tasks (including coordinating tasks) performed by LS-OPT during the design optimisation process

LS-OPT is set-up beforehand by the user to carry out the coordinating tasks depicted in Figure 5.2 and explained above. The user sets up a command file (which is similar to a script file) that is interpreted by LS-OPT at each design iteration, orchestrating all the necessary run-commands. The operating system used in these command files is UNIX or more specifically Linux.

Refer to section 5.5 for an example of such a command file.

5.2 Candidate objective and constraint functions

The standard mathematical optimisation problem concerns the minimisation of an objective function with respect to design variables subject to certain constraints. When defining a mathematical optimisation design problem, the choice of objective function and constraint function(s) is crucial to the success of the design optimisation

process. The selection of design variables also requires some insight into the possible sensitivity of parameters defining the design. Some of these parameters become variables in the design if they are deemed to influence the quality parameter or objective function significantly, in other words, if their variation would improve the design. Improving the design means that the value of the chosen objective function improves (thus becomes less, owing to the fact that the objective function is chosen in such a way that it needs to be minimised).

The SEN plays a major part in the continuous casting process explained in Chapters 2 and 4. As the SEN introduces the flow to the mould, it has an effect on the flow pattern in the mould; consequently **the SEN has an impact on the quality of the steel**. The SEN, in particular the SEN geometry, has a primary influence on the flow pattern: the SEN controls the speed, direction and other characteristics[4] of the jet entering the mould.

However, in the continuous casting steel making industry, the definition of quality is not straightforward, mainly because it depends largely on the type of product being cast and the manufacturing practices being followed. Consequently, defining parameters and/or flow situations (objective functions) that are desirable, is a difficult task. For the purpose of this study, quality is defined as the "internal cleanliness" of the steel, implicating that a stable meniscus surface is required for a constant casting speed. The stability of the meniscus surface becomes critical, especially when high casting speeds are considered.

In fact, previous studies [54] investigated the effect of static magnetic-field application on the mould in order to suppress the fluctuations of molten steel at the meniscus, and to provide uniformity of downward flow in the lower part of the mould. Too much fluctuation (instability) of the meniscus enhances slag powder entrainment. Entrained slag (or slag powder) is detrimental to the quality of the steel, as it solidifies within the slab and results in defects within and even on the surface of the final

[4] Other characteristics of the jet emanating from the SEN may include turbulence effects, the occurrence of vortices, jet angle as it exits from the SEN, impingement point onto the narrow mould wall, impingement angle, etc.

product. Thus, minimising the maximum turbulent kinetic energy on the meniscus surface is a good initial objective function in order to ensure meniscus stability.

There is, however, a contradictory constraint on the relative intensity of meniscus activity (resulting from upward and downward flows within the mould). The advantages of a very stable meniscus were discussed above; however, meniscus freezing may occur with possible catastrophic consequences [54]. Kubota *et al.* [55][56] proposed an optimum range of surface velocities (between 0.15 and 0.25 m/s) to minimise surface defects on sheet metals while preventing meniscus freezing. The possible existence of this optimum flow will be explored and investigated when the effect of temperature is linked to this optimisation process later in this Chapter. However, for the purposes of this study, the author assumes that meniscus freezing will not occur.

From the premise that "good quality" refers to the internal cleanliness of cast steel, other objective functions to consider for later optimisation studies include:

- minimising path lines that exit at the bottom of the mould
- maximising particle entrapment by the slag layer on the meniscus
- minimising the exit of the particles at the mould exit
- maximising the magnitude of the vortices or the barrel-roll effect of the steel jet as it impinges the mould wall, to ensure Ar-bubbles are drifted upwards, simultaneously limiting excessive meniscus movement (for the case where Argon is injected to manipulate the SEN jet and to prevent SEN port clogging).

Inter-relatedness of objective and constraint functions

The above paragraph (especially the last objective (and constraint) functions) illustrates the inter-dependency of the choice of objective and constraint functions. Practical design optimisation studies seldom produce meaningful results without cleverly chosen constraint functions.

For example: Suppose the objective function is to minimise the maximum kinetic turbulent energy on the meniscus. With no constraint functions, the mathematical

optimiser would obviously suggest a SEN design with a downward angle, a substantial submergence depth and large nozzles, until the objective function is practically zero. Moreover, without any constraints, the "optimum" SEN design's downward angles and oversize nozzles may be unmanufacturable (due to lacking material properties).

Thus; in order to extract some value from the optimum design, meaningful and carefully considered constraint functions must be chosen. In this example, the first obvious constraints will be physical constraints on the design to ensure that the optimum SEN can be manufactured. Secondary constraints necessary to achieve a meaningful practical design will probably be to limit the meniscus velocity, to prevent meniscus freezing, and to limit stationary spots on the meniscus surface, amongst others.

Refer to section 5.5 where the objective functions and constraint functions are formulated for the 2D design optimisation.

5.3 Design variables x

The importance of correctly chosen design variables cannot be over-emphasized. The selection of design variables also requires some insight into the possible sensitivity of parameters defining the design. Moreover, the choice of design variables is also influenced by the objective and constraint functions, as certain parameters are more dependent and linked to certain flow phenomena – represented by the functions in question.

During the parameterisation of the SEN geometry and mesh necessary for automation (section 5.1), a number of parameters (that can easily be altered) were identified. However, some parameters are operational parameters (and subsequently do not alter

the SEN design), and other design parameters might have an insignificant effect on the flow field.

Thus; the user needs to select design variables from the available parameters in a design optimisation study that will deliver the most effective improvement (depending on objective function) results.

As explained in section 5.1, the design variables $\boldsymbol{x}$, can be expressed as:

$$\boldsymbol{x} = \begin{bmatrix} x_1 \\ x_2 \\ \dots \\ x_n \end{bmatrix}; \text{ with } n \text{ design variables}$$

The values of the design variables $\boldsymbol{x}$ describe the design. Using the example in section 5.1 (refer to Figure 5.1), the design variables describe the SEN design (2D) with respect to the SEN port angles, SEN port heights, inherent well depth inside the SEN, and submergence depth of the SEN below the meniscus.

The optimum design, will be the values of $\boldsymbol{x}^* = [x^*_1 \; x^*_2. \; x^*_3 \dots \; x^*_n]$, which should be the optimum design of at least the 3rd design iteration[5] (equivalent to $\boldsymbol{x}^{(4,0)}$ or the 'base case' of the fourth design iteration according to definitions in section 5.1).

Scaling of design variables and constraints

In the event that the values of design variables differ in three orders of magnitude or more, it is advisable that the formal optimisation problem be set up in such a way that the values of the variables are scaled to similar orders of magnitude. LS-OPT scales design variables automatically in the event of optimisation variables differing in orders of magnitude. On the other hand, constraint functions are not scaled automatically. It is therefore recommended that different constraint functions are of similar orders of magnitude to ensure equal weight during the optimisation process, especially in the treatment of multiple violated constraints.

[5] A meaningful optimum design will not necessarily be reached after three design iterations: past experience only indicates that at least three design iterations were necessary for a meaningful improvement in the design.

5.4 Optimisation process

Apart from the coordinating ability of LS-OPT (to enable automated design optimisation as described in section 5.1.2), the "heart"/essence of LS-OPT is obviously its mathematical algorithms to predict the optimum design from the results of a number of CFD model evaluations.

LS-OPT uses a Response Surface Methodology together with a mathematical optimising algorithm (Snyman's LFOPC), and has certain advantages above other approximation methods[6]: [57]

- Design rules based on global approximations
- Does not require analytical sensitivity analyses
- Smoothes design response and stabilises numerical sensitivities
- Less function evaluations required due to accurate design surfaces in sub-regions, and trade-off curves and variable screening developed interactively

Existing and classical gradient-based optimisation algorithms do not perform satisfactory with real-world problems. This is particularly applicable to the field of engineering, where unique difficulties prevent the general application of general optimisation techniques. These optimisation difficulties that arise typically are:

- The functions are very expensive to evaluate (especially time-consuming with CFD simulations)
- The existence of noise (numerical or experimental) in the functions
- The presence of discontinuities in these functions
- Multiple local minima in these functions exist, requiring a global optimisation technique – as the response surface methodology
- The existence of regions in the design space where the functions are not defined

[6] An approximation is regression in essence, where a suitable mathematical function (curve in 2D or surface in 3D) is approximated over a pre-determined number of design points (values of objective function in terms of design variables $\boldsymbol{x}$).

- The occurrence of a large number of design variables, disqualifying certain classical optimisation methods (as sequential quadratic problems, for example)

LS-OPT therefore employs the successive region scheme (or successive response surface methodology) combined with an optimisation algorithm of Snyman to find the global minimum of the chosen objective functions, simultaneously satisfying the constraint functions.

5.4.1 Response Surface Methodology

In essence, response surfaces can be described as the approximations of experimental design points in smaller design spaces (also called regions of interest or sub-regions). Their (initial) sizes are determined by the ranges of variables chosen beforehand. Linear (or quadratic, depending on the accuracy required) approximations (called response surfaces) are fitted in these sub-regions. With each successive design iteration, these sub-regions are adjusted (reduced or moved) until the optimum design is found. Any optimisation algorithm can be used to evaluate these response surface approximations. As already mentioned, LS-OPT uses Snyman's Leapfrog and penalty function method (LFOPC) [14] to determine the optimum design on each response surface. The latter is called the optimisation algorithm.

Firstly, the most important terminology associated with the response surface methodology will be explained. Refer also to Figures 5.3 to 5.6 for visual representation (only 2 design variables) of these terminologies.

- *design space*: global ranges of design variables. With two design variables a design space can be illustrated as an area.
- *response surface*: mathematical approximation (linear or quadratic in LS-OPT) of experimental design points in region of interest or sub-region
- *design point*: value of objective function, where the objective function is expressed in terms of the design variables

- *regions of interest or sub-regions*: ranges of variables in which response surfaces are approximated. With 2 variables, it can be illustrated as smaller areas inside the total design space area.

Figure 5.3 represents the design space with the initial region of interest (with pre-determined variable ranges) inside it. The "baseline design" (Figure 5.3) is equivalent to the base case design as explained previously. The experimental design points are the chosen perturbations within the pre-determined and chosen ranges of design variables.

Figure 5.4 illustrates (example with only 2 design variables) how a response surface is approximated through the base case and experimental (perturbations) design points. The least squares method of approximating response surfaces is employed by LS-OPT. The LS-OPT user has three (3) options of basis functions for the response surface approximations:

- First-order approximation: linear
  The cost of first-order approximations is approximately n (using n design variables)
- Second-order approximations:
  - Full quadratic: cost $\approx n^2$
  - Elliptical approximation: cost $\approx 2n$

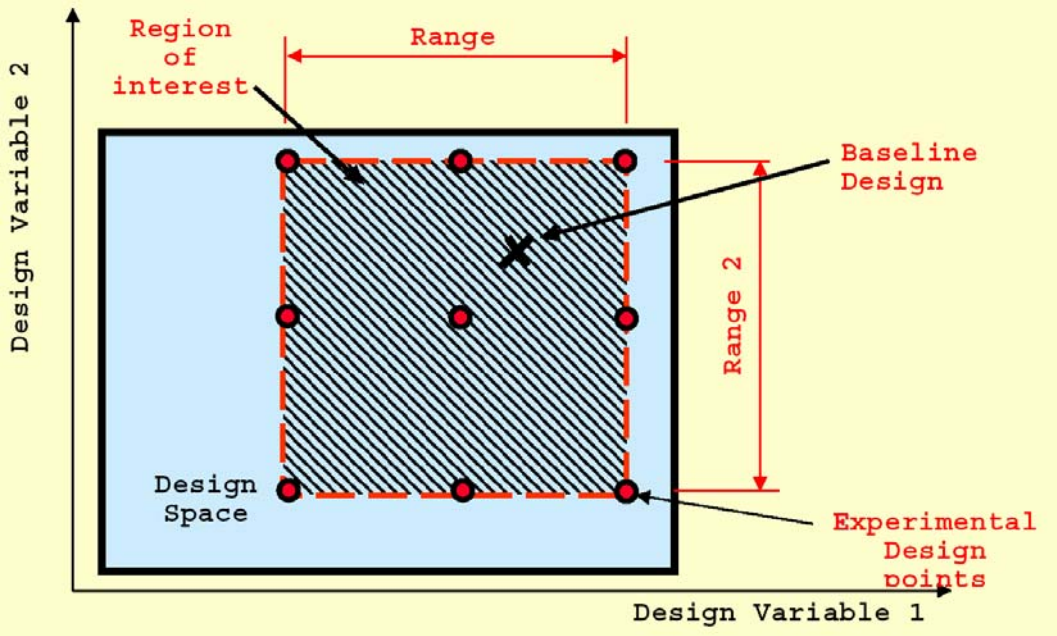

Figure 5.3: Design space terminology (design space, region of interest and experimental design points): response surface methodology [57]

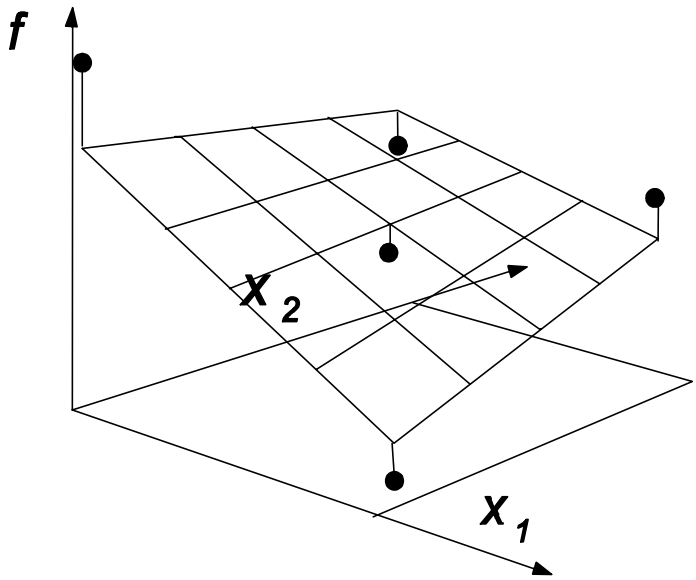

Figure 5.4: Example of response surface approximated over experimental design points [57]

The successive response surface approximation takes place on different (or rather adjusted) sub-regions, depending on the predicted optimum design point of the previous design iteration. The sub-regions (or successive regions of interest) can either “pan” (move) or “zoom” (reduce), or simultaneously pan and zoom. These adjustments are best described referring to Figure 5.5:

- pan: previous optimum predicted on the boundary of the region of interest of the previous design iteration
- zoom: previous optimum predicted close to the base case design point of the region of interest of the previous design iteration
- simultaneous pan and zoom: previous optimum predicted inside the boundary of the region of interest of the previous design iteration

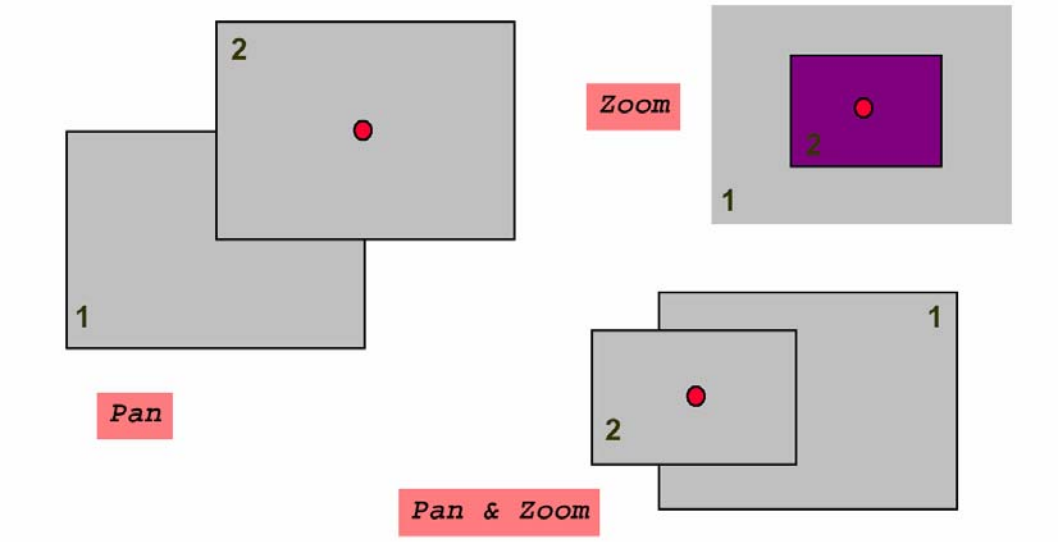

Figure 5.5: Successive sub-region reduction scheme [57]

Finally, Figure 5.6 illustrates the entire successive response surface methodology: The first region of interest is chosen (ranges of design variables pre-determined) around the starting design point (base case design). The second region of interest (that of the second design iteration) is panned, while that of the third and fourth design iterations are panned and zoomed – until an optimum design is found.

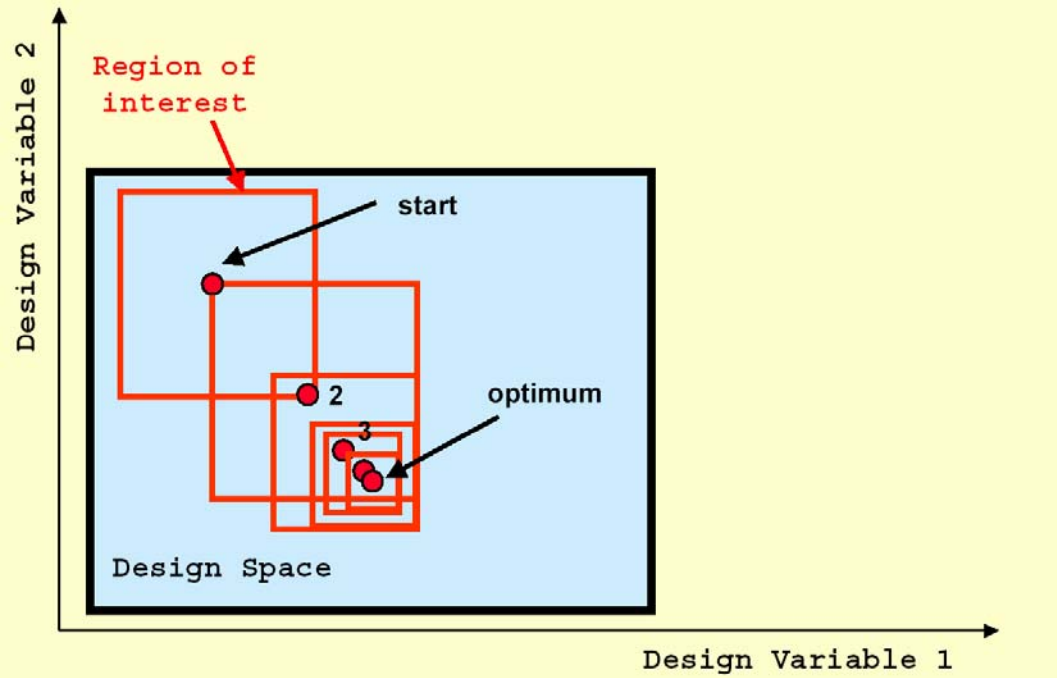

Figure 5.6: Successive sub-region reductions combined with optimisation of response surfaces (not shown) converges to an optimum [57]

5.4.2 LS-OPT Optimisation algorithm: LFOPC

The Leap-frog Method for Constrained Optimisation (LFOPC of Snyman) [14] is also known as the dynamic trajectory optimisation method, which is based on a physical model of a unit mass (ball) in a gravitational force field with a certain starting potential energy. After fitting an approximation or response surface to the experimental points inside each successive sub-region, the LFOPC algorithm is used to predict the optimum on the response surface in question.

The LFOPC algorithm is gradient-based, and also boasts the following characteristics:

- it uses only objective function *gradient* information or ∇f ;
- no explicit line searches are performed;
- it is robust, handling steep valleys, discontinuities and noise in the objective function and its gradient vector with relative ease;

- it seeks relative low minima and is thus suitable for global optimisation (although not a necessity with cleverly chosen starting regions of interest);
- it solves constrained optimisation problems using a penalty function formulation.

Penalty function formulations of a constrained optimisation problem forces the minimum of the unconstrained problem to also satisfy the inequality and equality constraint functions. More detail regarding the exact formulations and stages of penalty function applications can be viewed in Reference [14].

5.4.3 Variable screening (ANOVA)

After each design iteration, LS-OPT performs an analysis of variance (or ANOVA) on all responses to determine the significance of each response with respect to each variable. Significance of variables is a measure of their contribution towards change (improvement or deterioration) of each response.

Other measures of significance:
Variables with small gradients are designated as less significant. Noisy variables that display large scatter also reduce their significance.
The measure of significance used by LS-OPT is the lower bound of the 90% confidence interval of the regression coefficient b_j, or rather $b_j - \frac{\Delta b_j}{2}$. If this lower bound is close to or smaller than zero (0), the regression coefficient is regarded as insignificant. In a linear approximation, a variable can be removed if its coefficient is insignificant.

For more information on obtaining the regression coefficient b_j, and the type of distribution functions used to determine the confidence intervals, please refer to the LS-OPT manual and theory references [12][57].

Usually, before attempting an optimisation exercise, it is advisable to firstly only run the base case and a few perturbations to allow LS-OPT to evaluate the significance of the design variables. The obvious result of an ANOVA analysis is the reduction of variables without influencing the optimum value of the objective function. In other words, the optimum value of the objective function using only significant design variables compares favourably with the optimum of the objective function using all the variables [58].

5.5 2D Optimisation: An example of the design optimisation process

5.5.1 Objective and constraint functions

Following the explanations in section 5.2 concerning typical objective functions for a 2D SEN design optimisation, the objective function is formulated as follows: In an effort to improve the internal cleanliness of the cast steel in the mould, the meniscus activity will be limited to prevent the entrainment of slag. This will be achieved by minimising the maximum turbulent kinetic energy on the mould meniscus.

Typical constraint functions will be limiting the design parameters to be physical possible (manufacturable) SEN designs, as well as ensuring that the impact point is above the mould outlet (to prevent obvious break-outs). Another geometrical constraint is the linking of the SEN port angle to the submergence depth, thus prohibiting the occurrence of a jet impinging directly into the meniscus.

In an effort to prevent slag entrainment due to excessive velocity on the meniscus, the maximum average velocity on the meniscus is constrained to a maximum of 0.6m/s, as proposed by Kubota *et al* [56].

On the other hand, in an attempt to prevent meniscus freezing, the minimum meniscus temperature will be monitored and constrained to remain above the solidus temperature of the steel used in this optimisation study (1728K or 1414ºC).

5.5.2 Design variables *x*

Amongst the many design parameters in SEN design, the following parameters were selected as design variables for this optimisation study owing to their dominant effect on the flow pattern and their relevance to the current 2D application; *i.e.*, nozzle port angle, nozzle port height, and well depth. Although the submergence depth of the SEN was chosen as a variable in a previous optimisation study, it was decided to choose a constant 200mm submergence depth, mainly because it is regarded as an operational parameter rather than a design parameter. The submergence of the SEN is altered in any event during casting conditions as the SEN wall is eroded at the meniscus surface. Thus; a specified submerged depth below the meniscus will thus be of little use to a steel plant. Refer to Figure 5.1 (in section 5.1) for the definitions of these optimisation variables, with the exception of the submergence depth as a design variable.

Other typical SEN design parameters (not used in this study as variables) include: total length of SEN, amount of nozzle ports, geometrical shape of nozzle ports, radii of nozzle port corners, inner wall roughness of SEN, Argon gas injection rate (if present in order to counter clogging), to name a few.

Other operational parameters are kept constant for this optimisation study, and are listed in Tables 5.1 and 5.2 below.

Table 5.1: Constant parameters used in optimisation study: geometrical and steel properties

Description	**Casting speed [mm/min]**	**Slab width [mm]**	**Submergence depth [mm]**	**Steel dynamic viscosity [kg/(ms)]**	**Steel solidus temperature [K]/[ºC]**	**Liquid steel density [kg/m^3]**
Constant value	1000	1575	200	0.0064	1725/1440	6975

Table 5.2: Constant parameters used in optimisation study: energy/temperature considerations

Description	**Mould walls temperature [ºC]**	**Heat flux from mould walls [W/m^2]**	**Inlet temperature [ºC]**	**Outlet temperature [ºC]**	**Heat flux from meniscus [W/m^2]**
Constant value	1450	-300 000	1485	1410	-60 000

The ranges (or bounds) of the design variables were chosen by the author to represent possible physical SEN designs. These bounds (shown in Table 5.3) are represented by the inequality constraints in the formal optimisation problem formulation. The initial design was the base case or starting "point".

The minimum well depth was limited to 0.1mm (as opposed to an obvious 0mm) due to problems encountered in the automatic grid generation process in GAMBIT.

Table 5.3: Ranges (or bounds) of SEN design variables and initial design for optimisation study

Optimisation variable	**Minimum**	**Maximum**	**Initial design**
x_1 : SEN port angle [º]	-25	25	15
x_2 : SEN port height [mm]	30	80	70
x_3 : Well depth [mm]	0.1	50	0.1

5.5.3 Formulation of Optimisation problem

The complete mathematical formulation of the optimisation problem, in which the inequality constraints are written in the standard form $g_j(\boldsymbol{x}) \leq 0$, where $\boldsymbol{x}$ denotes the vector of the design variables $(x_1, x_2, x_3)^T$, or rather (nozzle port angle, nozzle port height, well depth)^T, is as follows:

minimise $f(\boldsymbol{x})$ = maximum turbulent kinetic energy on meniscus surface

subject to:

$$g_1(\boldsymbol{x}) = x_2 + x_3 - 113 \leq 0$$

$$g_2(\boldsymbol{x}) = \text{point of impingement under meniscus} - 675\text{mm} \leq 0$$

$$g_3(\boldsymbol{x}) = x_1 - 15/70*\text{submergence} - 75/7 \leq 0$$

$$g_4(\boldsymbol{x}) = \text{average maximum velocity} - 0.6\text{m/s} \leq 0$$

$$g_5(\boldsymbol{x}) = \text{average minimum meniscus temperature} + 1725^{\circ}\text{C} \leq 0$$

$$g_6(\boldsymbol{x}) = -x_1 - 25 \leq 0$$

$$g_7(\boldsymbol{x}) = x_1 - 25 \leq 0$$

$$g_8(\boldsymbol{x}) = -x_2 + 30 \leq 0$$

$$g_9(\boldsymbol{x}) = x_2 - 80 \leq 0$$

$$g_{10}(\boldsymbol{x}) = -x_3 + 0.1 \leq 0$$

$$g_{11}(\boldsymbol{x}) = x_3 - 50 \leq 0$$

} bounds of design variables

where:

- The ranges (or limits) of the design variables (see Table 5.3 and g_6 to g_{11}) are chosen in order to constrain the optimisation process to ensure a physically possible optimum.
- The inequality constraint g_1 is required to ensure a physically or geometrically possible SEN design (due to manufacturing constraints). Refer to Figure 5.1 to note that the sum of the SEN port height (x_2) and the well depth (x_3) may not exceed 113 mm.
- The constraint g_2 prohibits the impingement point to be more than 675 mm below the meniscus surface. Most continuous caster moulds currently used at Columbus Stainless are 800 mm in length; however, at most only 700mm of the mould is in contact with the molten steel. If the impingement point is too low, *i.e.,* under the mould exit, where the unsupported shell (especially the narrow shell) is at its thinnest and weakest, the likelihood of bulging and breakouts will increase. A maximum value of 675 mm is chosen in order to compensate for different meniscus levels and still ensure that the impingement point remains above the mould exit.

- The constraint g_3 ensures that the jet never impinges the meniscus directly (with a large positive angle and the constant submergence depth), which will only result in the violation of the constraint g_4 that endeavours to limit the maximum meniscus velocity to 0.6 m/s. If a geometrical SEN design that will surely result in a violation of a constraint function (*i.e.*, g_4) can be avoided from the first instance, a precious (and computational expensive) CFD evaluation can be saved. The Optimiser is thus much more effective with the assistance of this constraint function.
- The constraint g_4 endeavours to limit the maximum meniscus velocity to 0.6 m/s in an effort to prevent slag entrainment.
- Constraint g_5 monitors the minimum meniscus temperature to ensure that this temperature remains above the solidus temperature of the steel. This will hopefully prevent meniscus freezing, which is also a serious cause of breakouts.

Note that constraints g_1 to g_5 were scaled using LS-OPT to ensure that all the violations of the constraint functions are of the same order. This will prevent constraint functions with larger violations from dominating the Optimiser's choice of perturbations during the optimisation exercise.

5.5.4 Base case: discussion

As described in previous chapters in this dissertation, the base case design needs to be set up and confirmed or validated before commencing with the optimisation study.

The 2D base case was developed and validated in Chapter 4. For the sake of completeness, the basic CFD modelling is repeated:

5.5.4.1 Geometry and Mesh for 2D

Due to symmetry, only half of the SEN and mould is modelled by applying a symmetry plane (or edge for 2D) on the centre plane of the mould. It is known that the flow is non-symmetrical when a slide gate valve is used upstream of the SEN in order to control the meniscus height and casting speed [4][5]. However, when using a stopper as a control valve (which is the case at Columbus Stainless), the flow is generally more symmetrical and thus assumed to be symmetrical for the purposes of this design study.

The grid for the 2D half-model SEN and mould geometry is generated automatically for all the design iterations and perturbations using GAMBIT as described in section 5.1. A fine (high density), fully-structured grid is generated using quadrilateral (commonly known as "hex") cells. The mesh of the starting design configuration is shown in Figure 5.7 and consists of approximately 75 000 cells. Grid adaption was employed during each CFD evaluation; however, only in the jet regions and not throughout the entire mould.

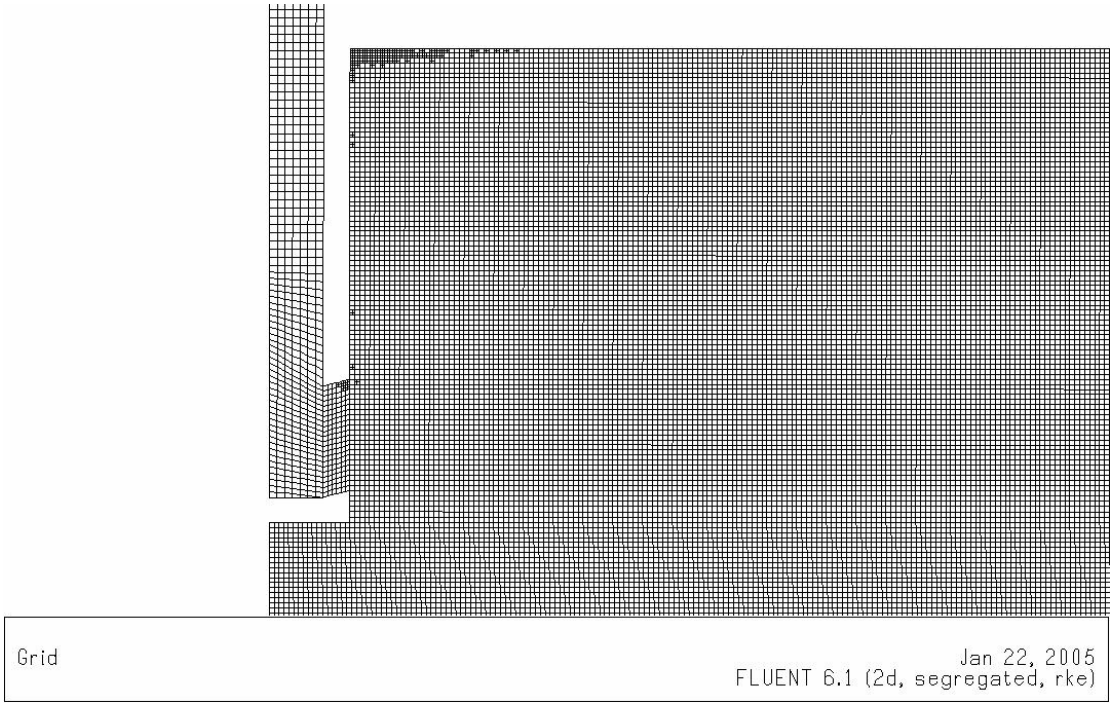

Figure 5.7: Structured mesh of SEN and mould 2D half-model

5.5.4.2 SEN nozzle height in optimisation study: 3D vs. 2D

The SEN port height shown in Figure 5.1 is the actual height of the 3D SEN port on the centre plane. However, when modelling a 2D SEN and mould, the jet is no longer modelled to be emanating from a hole, but rather from an indefinitely long slot. Observing the shape of the 3D nozzle (from the side) in Figure 5.8, it is clear that the height of the slot must be reduced to be compared to the 3D nozzle. Taking into account the radius of the upper and lower curve and the width of the nozzle hole (which was coincidentally held constant for this study), the average height is computed analytically (integrated along the radius) for each grid generated during each design iteration, as shown in Figure 5.8. The average height of the 3D nozzle therefore becomes the 2D nozzle (or rather slot) height, in order to achieve more accurate 2D results, which will hopefully be more comparable with the results of similar 3D CFD models.

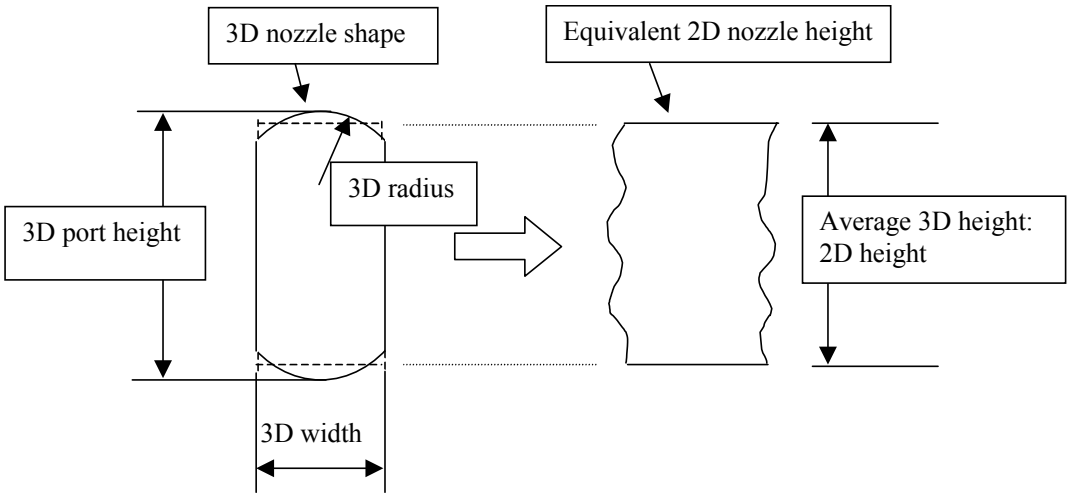

Figure 5.8: Side view of the 3D SEN nozzle and subsequent reduction of port height for average height (2D height)

5.5.4.3 Boundary conditions

A slip surface (zero shear stress) is used on the upper boundary of the steel (*i.e.,* the meniscus surface) to model the slag layer as indicated in Figure 5.7. The narrow mould wall is modelled as a moving wall, moving downwards at the casting speed as indicated in Table 5.1. The bottom of the mould is modelled as a pressure outlet boundary condition at atmospheric pressure. The length of the mould is modelled as approximately 4.1 meters, which is more than is required (approximately 3m [2]) to model both recirculating zones.

5.5.4.4 Solver solution procedure

A similar solution procedure as described in Chapter 4 was used to achieve converged results. The only difference is that when grid adaption takes place, it only takes place in the jet region, and not throughout the entire mould as implicated in Chapter 4. Sufficient convergence is assumed when at least a four-order drop in all normalised residuals are achieved.

5.5.5 Automation for design optimisation

As explained in section 5.1 above, the following script files were developed as soon as the base case design CFD model were validated and trustworthy, in order to automate the design optimisation process:

- GAMBIT script file
- FLUENT script files
    - Set-up file
    - Run file
- LS-OPT command file

5.5.5.1 GAMBIT parameterised script file

Refer to Appendix J for the GAMBIT script file for the generation of all possible designs within the bounds of the design variables of this optimisation

study. Section 5.1 explains the fundamental concepts behind parameterised geometries and how to create any geometry using script files.

5.5.5.2 FLUENT script files

a) Set-up file

b) Run file

Usually these two script files are combined into one FLUENT script file, as the second set of tasks (run file) naturally follows the set-up procedure. Refer to Appendix K for the combined FLUENT script file as used in this optimisation study:

- set-up section,
- followed by the run section.

Section 5.1 explains the fundamentals behind the automatic manipulation of the CFD solver FLUENT using script files.

5.5.5.3 LS-OPT command file

The command file has all the information concerning the optimisation exercise, including the variables and their respective bounds, as well as all the run commands for GAMBIT and FLUENT.

Refer to Appendix L for the command file (com-file) used for this optimisation exercise.

5.5.6 Results and discussion of design iterations

5.5.6.1 Flow and Meniscus Turbulent Kinetic Energy Results: base case

The flow pattern of the initial design (or base case design) is shown in Figure 5.9. The constraint g_2 is also shown in Figure 5.9, as well as the approximate mould exit. The velocity magnitude of the vectors is indicated by their relative lengths with respect to the 1 m/s vector shown in the same figure, as well as the colour scale.

Note that the impingement point for the base case is well above the lowest allowable point; however, there is believed to be still much room for improvement for the maximum Turbulent Kinetic Energy (henceforth TKE) on the meniscus surface.

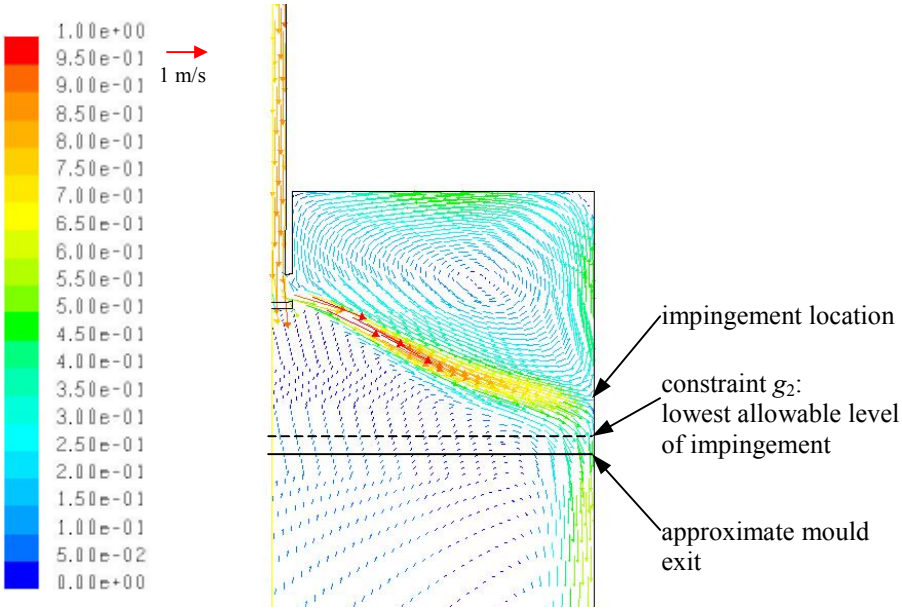

Figure 5.9: Flow pattern (velocity vectors) and point of impingement of initial design

5.5.6.2 Optimisation History

The optimisation results are shown in Figures 5.10 to 5.12. The optimisation history of the objective function (maximum TKE) is shown in Figure 5.10. The optimisation history of the maximum velocity on the meniscus is also shown in the same figure, showing the interdependence of the maximum TKE and velocity on the meniscus. The optimisation history of the constraint

functions g_1 and g_3 (in millimetres) is shown in Figure 5.11, while that of the design variables is shown in Figure 5.12.

The only active constraint function was g_4, which monitored the minimum meniscus temperature. Although the constraint functions g_1 and g_3 in Figure 5.11 were never active at the design points (thus equal to or smaller than zero), it contains some telltale information regarding the optimisation process. After the first design iteration, the Optimiser enlarged the port height to its maximum bound, which is reflected in the fact that g_1 moves closer to zero as the design nears the manufacturing limit. However, throughout the optimisation process, g_1 never becomes active – all the designs are thus manufacturable. The constraint function g_3 follows the same trend as the port angle (in Figure 5.12), owing to the fact that they are linked algebraically: the lower the port angle, the likelihood that the jet will impinge directly into the meniscus, is reduced (and therefore the g_3 will be even more negative).

Interestingly, the optimisation process initially moved in the "wrong" direction, exploiting a design with an upward port angle design (iterations 1 to 3). From the fourth design iteration, a much smaller port angle was suggested by the Optimiser (Figure 5.12), with positive results: the maximum TKE on the meniscus was reduced significantly (Figure 5.10). As can be seen in Figures 5.10 to 5.12, further reductions of the port angle also resulted in the reduction of the maximum TKE.

The well depth was also enlarged only from the third design iteration, with success, as the maximum TKE was simultaneously reduced. This can be attributed to the fact that the well accelerates the dissipation of turbulent energy, resulting in a less concentrated jet.

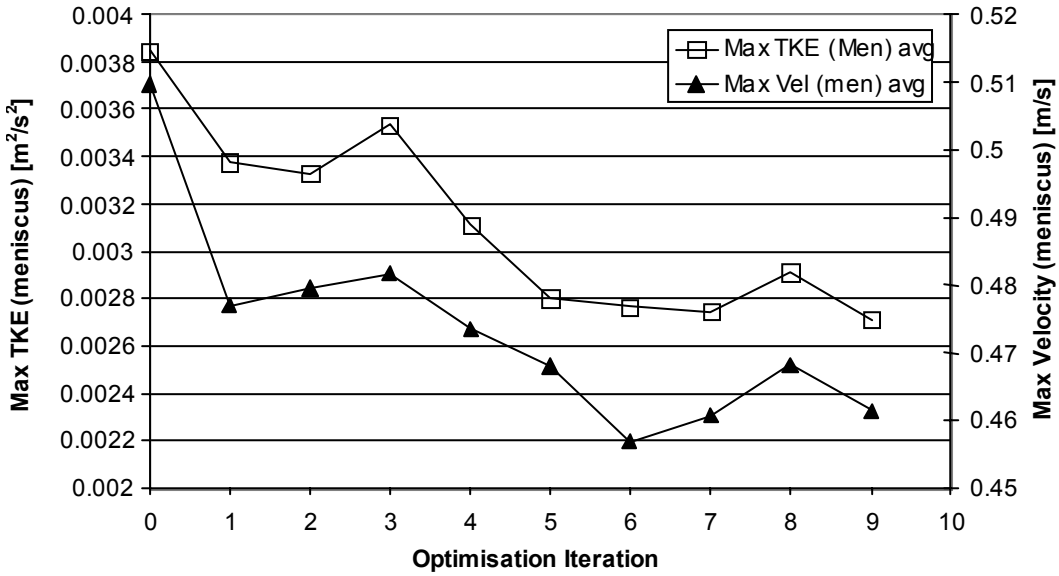

Figure 5.10: Optimisation history: Objective function (max TKE) and maximum velocity on meniscus

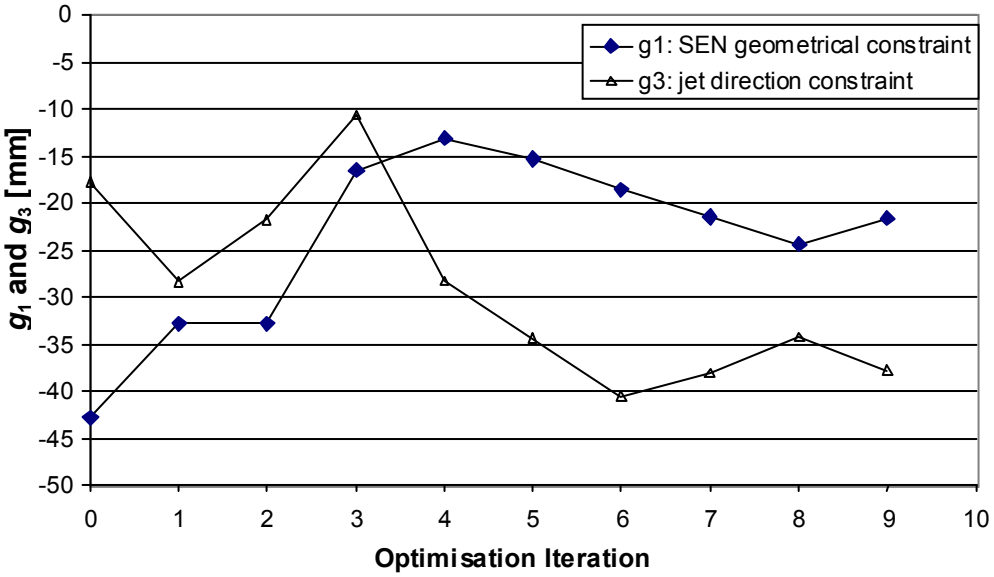

Figure 5.11: Optimisation history: Constraint functions g_1 (geometrical constraint) and g_3 (jet direction constraint)

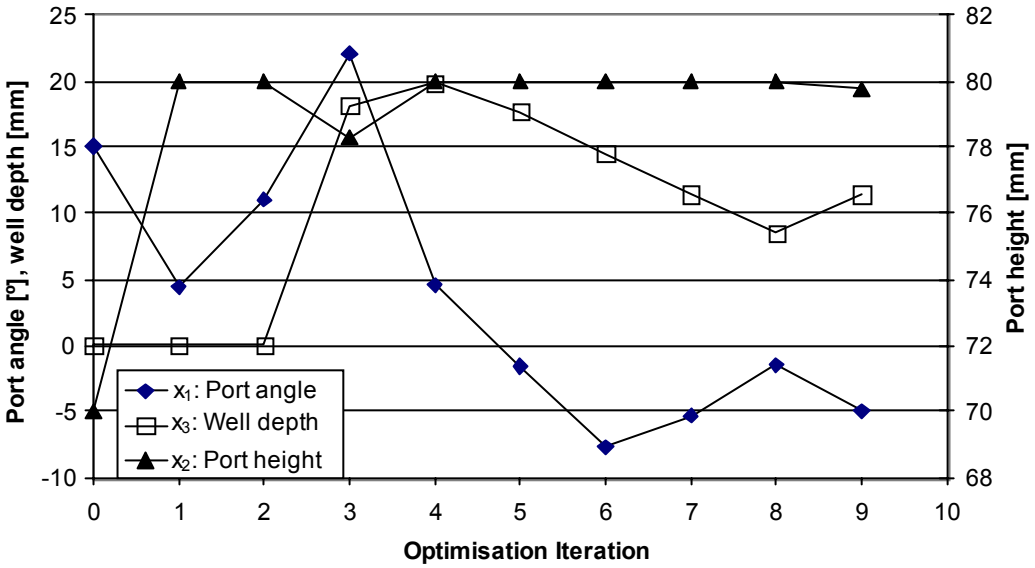

Figure 5.12: Optimisation history: Design variables

The Response Surface Method used by the Optimiser, generates 7 designs ($\boldsymbol{x}^1$ to $\boldsymbol{x}^7$) for 3 variables with each design iteration on the response domain [13], using the CFD solver to evaluate the objective function value for each design. A response surface (a linear surface for this study) is then fitted through these objective function values using the minimum error of the root mean squared – approach as explained in preceding sections. It is thus inevitable that extremely good or extremely bad designs (outliers) are discarded when using the Response Surface Method, especially when linear surfaces are used. However, these auxiliary designs are recorded and the best design (although not the optimum of the optimisation process) can surely be considered as an optimum design. In this optimisation exercise, however, the optimum design predicted by the optimiser was used.

5.5.7 Optimum design with design variables $\boldsymbol{x}^*$

The optimum SEN design is considered to have been reached after 9 design iterations. The optimum design in terms of its design variables is displayed in Table 5.4, where a summary of the design optimisation results is shown. The

design variables of the optimum design in Table 5.4 have been rounded to the first decimal.

Table 5.4: Summary of design optimisation results

Case	**x_1 : SEN port angle [°]**	**x_2 : SEN port height [mm]**	**x_3 : Well depth [mm]**	**Max. TKE on meniscus [m^2/s^2]**	**Impingement point below meniscus [mm]**	**Max. velocity on meniscus [m/s]**
Initial	15	70	0.1	0.003847	521.99	0.5097
Optimum (x^*)	-5.0	79.8	11.5	0.002709	570.38	0.4614

The TKE on the meniscus surface of the initial design and the optimum design are plotted and compared in Figure 5.13. An improvement of 29.6% was achieved with the optimum design over the initial design, reducing the maximum TKE from 0.003847 m^2/s^2 to 0.002709 m^2/s^2. Note that the TKE on the meniscus is spread more evenly (although marginally) across the meniscus surface with the optimum design. This is thus a better design than the initial design according to Kubota *et al.* [56], who state that spreading the TKE over the meniscus surface while simultaneously reducing the maximum value, will reduce the chance of meniscus freezing in an inactive area and simultaneously reduce the likelihood of slag entrainment.

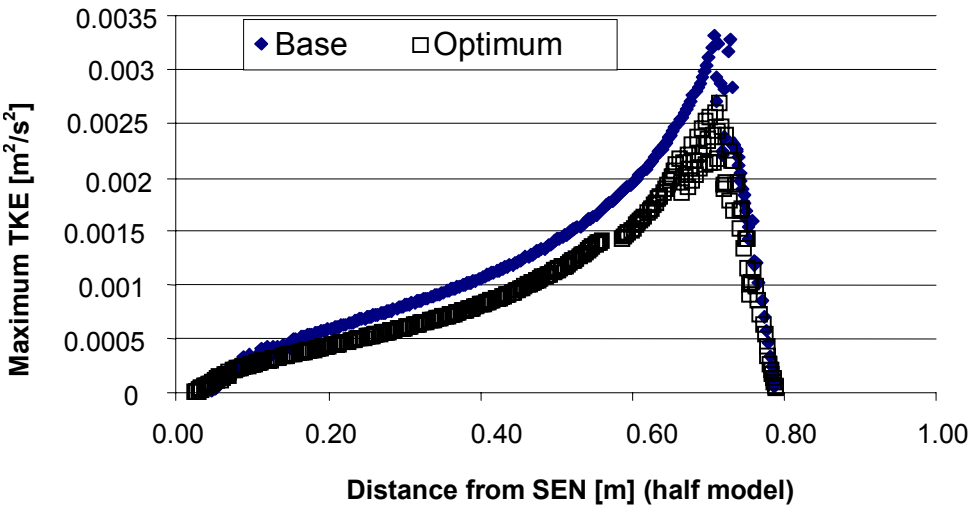

Figure 5.13: Comparison of turbulent kinetic energy on meniscus surface between initial design and optimum design (2D half model)

Figure 5.14 compares the flow pattern of the optimum design with that of the initial design. The colour scale in Figure 5.14 of the contours represents the TKE in the velocity flow field. The TKE content of the flow field is thus shown and the design improvement with respect to the objective function and impingement constraint are clearly visible at the meniscus surfaces (darker colours at or near the meniscus means less activity).

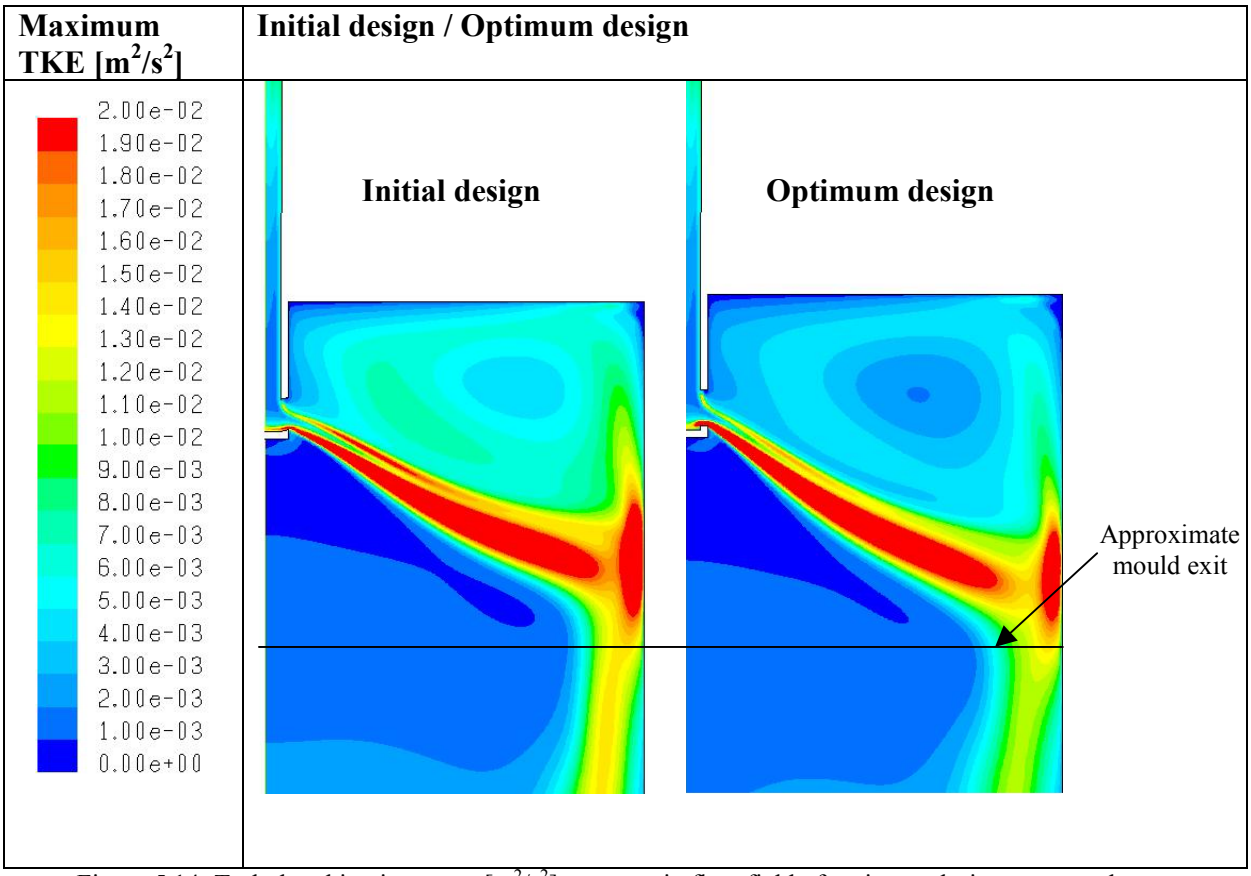

Figure 5.14: Turbulent kinetic energy [m^2/s^2] contours in flow field of optimum design compared with initial design

5.6 3D SEN optimisation: design space exploration

5.6.1 Computational expensive 3D modelling

Due to the computationally expensive 3D modelling, it is currently impossible to follow exactly the same procedure as in the previous 2D optimisation example (section 5.5).

Instead, a central-composite design method was followed to determine experimental points (similar to perturbations in normal LS-OPT optimisation

exercises). Using this method, an improved design can be estimated with much less CFD evaluations.

3D CFD simulations of the SEN and mould require considerably more computing power than 2D simulations, due to the following reasons:

More complex flow

The flow in 3D for a SEN and mould combination is much more complex than a 2D simulation, owing to the necessity of solving the Navier-Stokes equations in 3 dimensional space, as well as modelling turbulence in 3 dimensions. The isotropic turbulence assumption[7] of the k-ε turbulence (Realisable) models [10], which has proven to be quite accurate for 2D simulations, no longer delivers accurate and repeatable 3D solutions. The only turbulence model that does not assume isotropic turbulence is the Reynolds Stress Model (RSM)[8]. However, this model requires a much finer mesh than the k-ε or k-ω models.

More cells (3D) essential

During initial investigation phases, the base case SEN design (as described in Chapter 4) with a submergence depth of 200mm, and a mould width of 1575mm, was modelled using the RSM turbulence model. The mesh consisted of approximately 3 million cells. In order to ensure convergence, the CFD model iterated for several months on a 3 GHz Intel Pentium 4, reaching approximately 44250 iterations. This proves that the RSM turbulence model is not suitable for general optimisation use.

Using the computationally less expensive k-ω turbulence model, a coarser mesh can be used. Subsequently, a meaningful optimisation study can be performed in a much more acceptable time frame.

[7] Refer to Chapter 4 for discussion of different turbulence models, as well as the inter-relatedness of physically correct turbulence modelling and computational expensiveness.

[8] The RSM model requires that 7 equations be solved during each iteration, as opposed to only 2 equations of the k-ε or k-ω models. Refer to Chapter 4 for more information. LES (Large Eddy Simulation) requires such an extremely fine mesh, that it is not even considered as an option due to limiting computing power.

Apart from the fact that more computing power is necessary, another problem surfaced concerning sequential 3D CFD simulations:

Wide mould: jet instability and convergence problems

The author noticed that (especially 3D) CFD solutions of any SEN and mould model proved to be much more stable (including repeatable convergence of solutions) in the event of a reduced mould width. Coincidentally, the main THRIP partner, Columbus Steel, Middelburg, required an optimum SEN design for their 1000mm to 1300mm slab widths (narrow to medium), as casting speed was increased by approximately 30% (from 1m/min to 1.3 m/min) for these widths. This 3D design space exploration study will thus focus on a narrower mould width of 1060mm and 1250mm (as opposed to the widest width of 1575mm of the 2D optimisation study). These two widths have been selected, as they are representative for the 1000mm – 1300mm range. Moreover, full-scale water model validations [32] are available for these widths.

5.6.2 Design space exploration

5.6.2.1 General and design variables

The experimental points or designs (using the central-composite design method) were chosen for the following three design variables:

- port angle
- port height
- well depth

Owing to the 3-dimensional nature of the SEN, a few parameters were assumed to be constant with respect to the automatic geometry generation:

- upper and lower ports have the same angle
- port width remains constant
- port curvature (top and bottom) remains constant
- well angle remains constant at 0 degrees (in other words, the bottom of the well is flat)

For this 3D optimisation study (or rather design space exploration), the three design variables will be optimised using the "worst case" submergence depth of 80mm. The latter submergence depth is the shallowest depth used by Columbus Stainless during normal casting operations. It is regarded as the worst case due to more meniscus activity (increased turbulent kinetic energy) resulting from the proximity of the exiting molten steel jets. The increased meniscus activity invariably causes slag entrainment, reducing the quality of the cast steel and resultant slab quality. Furthermore, the shallow jets can also prohibit a well-defined bottom barrel roll, further contributing to inferior quality steel due to the absence of a vehicle to remove impurities from the cast steel in the mould cavity.

All other constant operational parameters for this exploration study are indicated in Table 5.5.

Table 5.5: Constant parameters used in 3D design space exploration optimisation study: geometrical and steel properties

Description	**Casting speed [mm/min]**	**Slab widths [mm]**	**Submergence depth [mm]**	**Steel dynamic viscosity [kg/(ms)]**	**Steel solidus temperature [K]/[°C]**	**Liquid steel density [kg/m^3]**
Constant value	1300	1060 and 1250	80	0.0064	1725/1440	6975

The CFD model is assumed to be accurate for this design space exploration exercise, as the CFD model of the base case was validated using water model results in Chapter 4.

5.6.2.2 Formulation of multi-objective function

The basic objective function for this design space exploration is to minimise the meniscus turbulent kinetic energy as well as to limit excessive meniscus velocity, for both widths (1060 and 1250mm). The submergence depth will of course be kept constant at 80mm. All the different chosen SEN designs will be evaluated for both widths.

A combined objective function (multi-objective function) is defined as follows to achieve the basic objective of minimising meniscus turbulent kinetic energy:

Multi-objective = (Max_TKE_1060 + Max_TKE_1250)*1000
+ (Max_maxVel_1060 + Max_maxVel_1250)*10

where:

Max_TKE_*width* : average[9] magnitudes of maximum turbulent kinetic energy on meniscus

Max_maxVel_*width* : average magnitudes of maximum meniscus velocity

Note that the maximum TKE values are multiplied by 1000, as opposed to only 10 for the velocity magnitudes, to ensure that the values are comparable (thus of the same order), preventing that only one factor dominates the multi-objective function.

5.6.2.3 Geometry and mesh (parameterisation of mesh)

The geometry was parameterised using the same principles as described in previous sections of this chapter. However, when parameterising 3D geometries, more complicated exceptions can occur during the generation of different geometries.

The author developed a 3D automatic geometry and mesh generator (consisting of a GAMBIT script file) based on the old Columbus SEN (without a well).

[9] Instability of the CFD solutions causes the maximum TKE to vary from one CFD iteration to the next, despite the fact that the residuals have fallen sufficiently for general convergence. Consequently, the values of maximum TKE (as well as that of maximum velocity) are extracted from the last few thousand iterations and **averaged** for a more representative maximum TKE (or maximum velocity) value.

The approach employed by the script file was: generating a full 3D model using volumes as geometric building blocks, and dividing it in quarters afterwards to obtain the desired quarter model. Unfortunately, this method created 3D volumes in the SEN flow field that cannot be meshed using stable quadrilateral cells, and tetrahedral cells (tet-cells) had to be employed. The use of tetrahedral cells has a negative impact on especially complex jet flows, and must be avoided to obtain repeatable and believable solutions, as explained in Chapter 4. An example of the GAMBIT script file used to generate a SEN design (without the well) can be viewed in Appendix M. This script file was never used for optimisation purposes, due to the unsuitability of the mesh.

However, as Columbus Stainless required a design suggestion using a welled SEN, a new parameterisation method was required. A colleague at the University of Pretoria followed a different approach: the 3D quarter model was built up from scratch, starting with vertices or points in space, connecting the latter to form lines, forming surfaces with these lines, and ultimately linking the surfaces to create volumes. Using this (elaborate) method, more elemental volumes could be created, enabling hexahedral cells to be used throughout the SEN volume.

In order to parameterise the well depth, a minimum well depth of 1 mm had to be accepted as sufficient for a no-well condition, as the GAMBIT script file could not handle a 0mm well depth. The latter GAMBIT script file (also known as a journal file) was used to generate the geometry and mesh for the different SEN designs chosen in this design space exploration.

This journal file is approximately 2200 lines long: the excessive length of the file is due to all the exceptions that can occur in the geometry for the range of parameters chosen. The splitting of faces[10] causes renaming by GAMBIT in a non-intuitive way, and the loops in the journal file in question test for these.

[10] Splitting of faces: a necessary operation in GAMBIT during face and ultimately volume creation.

The file generates a mesh of about 500 000 cells depending on the geometry that is the starting mesh for the dynamic mesh adaption[11] used in FLUENT. This means that the mesh is refined and coarsened as the solution proceeds based on velocity gradients (in this case). This is an attempt to follow the formation of the SEN jet with grid clustering. A maximum cell count of about 850 000 is reached in this process depending on the complexity of the flow field in each case.

5.6.2.4 Boundary conditions and other settings

The boundary conditions are similar to that in the 2D optimisation exercise section 5.5. For the sake of completeness, the typical boundary conditions specified in FLUENT for this design space exploration, are shown in Figure 5.15.

Other settings are also similar to the 2D optimisation study, as well as the FLUENT script files used to follow a certain solution procedure to ensure convergence of critical residuals.

[11] Dynamic mesh adaption: refer to Chapter 4 for explanations and discussions.

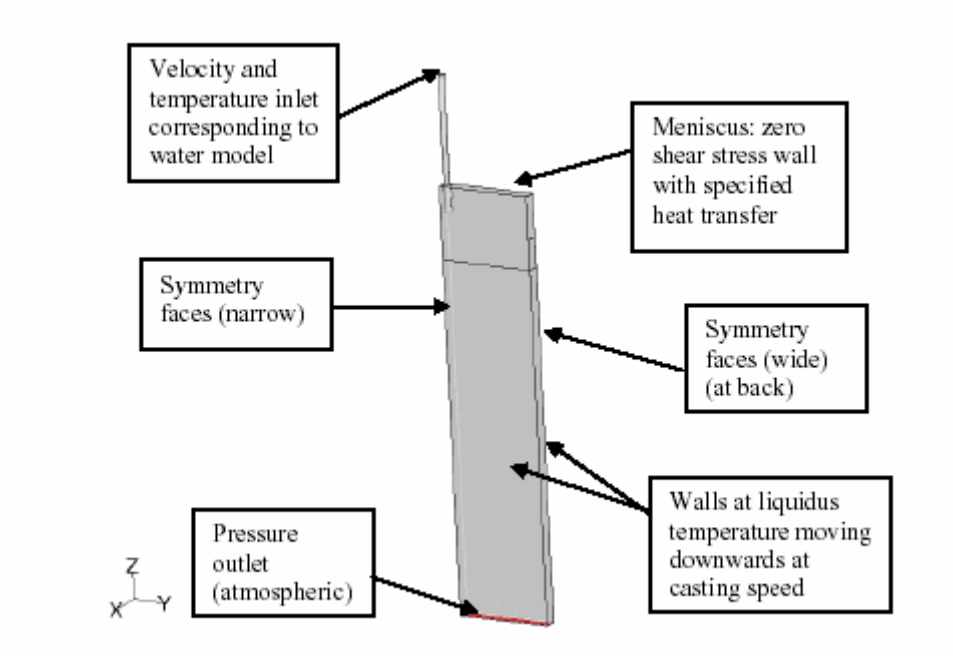

Figure 5.15: Typical boundary conditions for quarter model of 3D CFD SEN and mould model

5.6.2.5 Experimental design

A central-composite design was used in LS-OPT [30] for the three design variables considered, *i.e.*, port angle, port height and well depth. The old SEN design (base case design in Chapter 4) was added as experimental design point 1.0, or design $\boldsymbol{x}^{(1,0)}$ when using the same notation as in section 5.1.

All the experimental design points are listed in Table 5.6, including the base case (experimental design point 1.0) and the linear and quadratic optima fits as predicted by LS-OPT. Figure 5.16 illustrates the experimental design points listed in Table 5.6, simultaneously explaining the reason why this design is called central composite. The experimental points are chosen in the centre of the faces of the "design space" that was chosen by the user. The reason why "design space" is written in inverted commas is because the latter cannot be represented by a graph when there are more than 3 design variables. In this case it can be depicted diagrammatically as only 3 design variables are optimised.

Table 5.6: Experiments in central-composite design, including base case (experiment 1.0) and linear and quadratic optima fits by LS-OPT

Experimental design point	**SEN port angle [º]**	**SEN port height [mm]**	**SEN well depth [mm]**
1.0	15	70	$1 \approx 0$
1.1	0	55	20
1.2	7.9	69.9	32.1
1.3	-12.9	69.9	32.1
1.4	7.9	40.1	32.1
1.5	-12.9	40.1	32.1
1.6	7.9	69.9	8.9
1.7	-12.9	69.9	8.9
1.8	7.9	40.1	8.9
1.9	-12.9	40.1	8.9
1.10	-2.5	55	20.5
1.11	15	55	20.5
1.12	-2.5	80	20.5
1.13	-2.5	55	40
1.14	-20	55	20.5
1.15	-2.5	30	20.5
1.16	-2.5	55	1
2.0_linear	-20	80	1
2.0_quadratic	-20	55.56	40

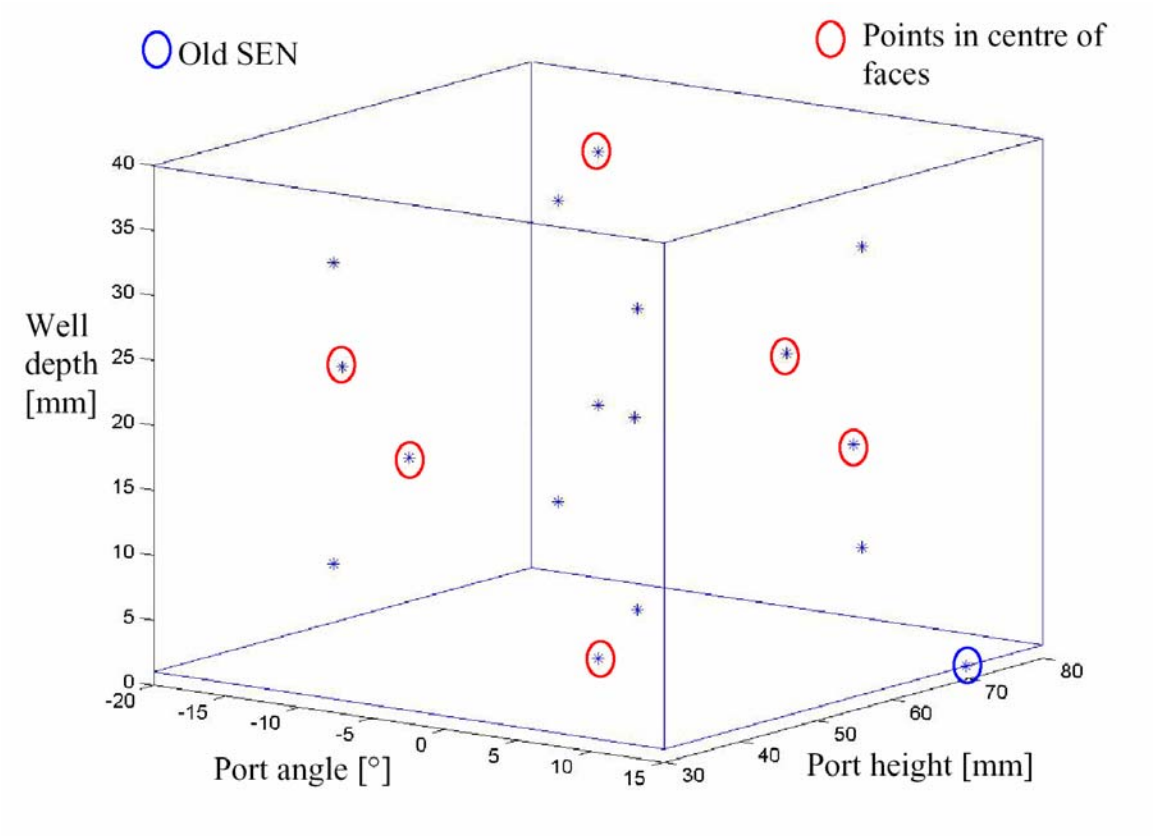

Figure 5.16: Central-composite design experimental points

5.6.3 Results: Design space exploration

Each experimental design point was evaluated using CFD techniques, as explained in Chapter 4.

All these CFD simulations (or evaluations) for all experimental design points as indicated in Table 5.6, were run for both slab widths (1060 and 1250mm), for a submergence depth of 80mm and a casting speed of 1.3m/min. Summary results[12] of all these cases can be viewed in Appendix N.

The values of the multi-objective function of the 19 experiments (Table 5.6) are depicted graphically in Figure 5.17. Note that the basic objective of this exercise

[12] Summary results (Appendix N) include an executive summary of the maximum TKE as well as the maximum velocity on the meniscus for both widths. Furthermore, the contours of magnitude of velocity on the symmetry plane of each CFD simulation (converged) are also shown so that the reader can evaluate the physical flow.

is to find a SEN design with the lowest multi-objective value. Consequently, the four designs that performed well (indicated in Figure 5.16 with red circles) are: experimental designs 1.0, 1.7, 2.0_linear and 2.0_quadratic.

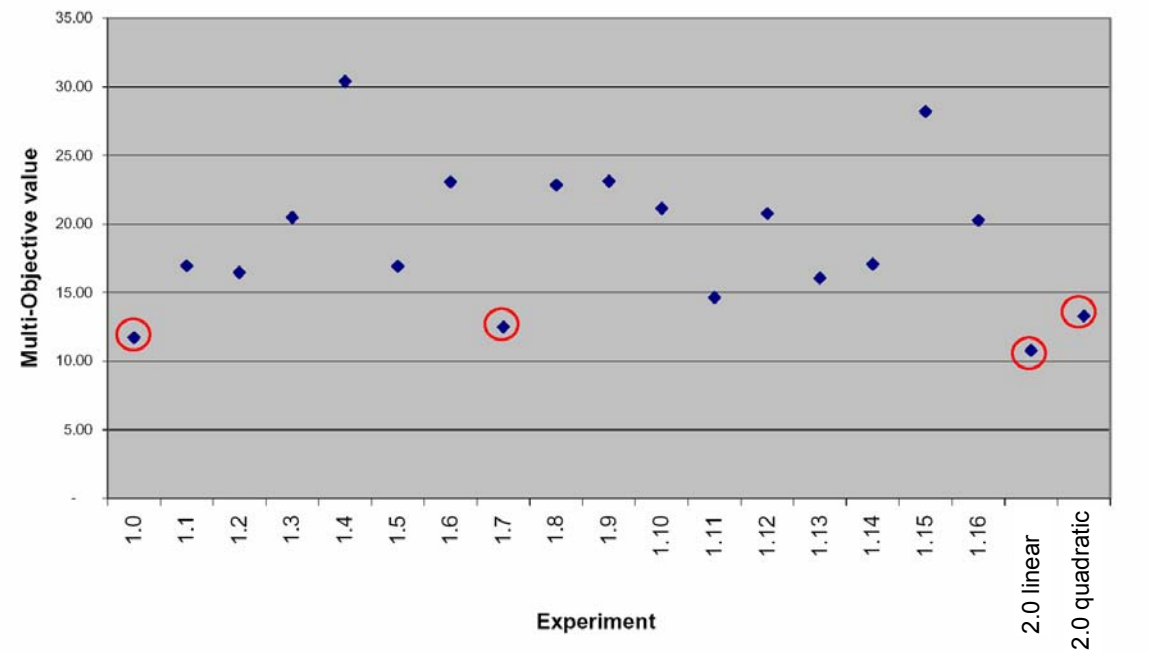

Figure 5.17: Multi-objective values of the experiments listed in Table 5.6

Considering the parameters of these designs, it can be seen that design 1.0 is the original Vesuvius SEN design (old SEN). Design 1.7 has a moderate well (9mm) and a downward angle of approximately 13º. Design 2.0_linear has a port height and downward angle as much as allowed with no well, while 2.0_quadratic has a moderate port height, with a maximum allowable downward angle and well depth.

The designs that performed the poorest (*i.e.*, 1.4 and 1.15) were those with small ports and medium to deep wells. From the data in Appendix N, these designs have very shallow SEN jets, derogating the meniscus stability due to jet proximity. The instability of the CFD solution can also be observed by just viewing the quite unphysical velocity contours of these poor performers (Appendix N).

In order to select the best SEN design from the four best performers, more detail information and flow displays were extracted from the CFD solutions. In order to

evaluate the four best designs, the following contours of the CFD solution models were generated for each design (for both widths):

- contours of velocity on the symmetry plane
- contours of helicity[13] on the symmetry plane
- contours of turbulent kinetic energy on symmetry plane
- contours of vorticity on the symmetry plane
- contours of shear stress on the wide mould walls
- contours of temperature on the symmetry plane
- path lines originating from the SEN inlet, coloured by vorticity magnitude

All these CFD results of the four best SEN designs are shown in Appendix O.

Considering the results in Appendix O, one often mistakes the flow as being similar to 2D flow, due to the customary display of the flow patterns on the symmetry plane of the 3D SEN and mould model. In order to demonstrate the 3-dimensional nature of the flow field, another display method is used: The jet is displayed in 3D by rendering iso-surfaces[14] of velocity magnitude coloured by turbulent kinetic energy. Refer to Appendix P for these displays of the four best SEN designs.

Of course, it is important to verify the robustness of the chosen SEN design. Factors that may influence the performance of the new SEN design are:

- Initial tolerance differences due to manufacturing tolerances and errors
- Gradual internal geometry variances due to clogging and the presence of impurities
- Operational parameter variations due to control inadequacies of the casting speed, for example

[13] Helicity was defined in Chapter 4, footnote 14 [10].
[14] An iso-surface of velocity magnitude (for example) is when only the surface area, where a specified constant velocity magnitude is achieved in the entire flow field, is displayed. Of course, other properties may vary over this iso-surface, as turbulent kinetic energy for example.

Refer to Chapter 6 (Future Work and Conclusion) for remarks on this emerging topic, which is applicable to practically all CFD optimisation design exercises.

5.6.4 Design space exploration: Geometry of chosen design

The chosen design is the optimum predicted using the linear approximation of LS-OPT. The 2.0_linear design performed marginally better than the other four designs in the multi-objective function.

The 3D SEN design thus recommended for manufacture for a plant trial is depicted diagrammatically with a 3D solid surface rendering in Figure 5.18. This SEN design (Table 5.7) should perform satisfactorily for widths ranging from 1000 – 1300mm, at a casting speed of 1.3 m/min.

Table 5.7: Chosen design following 3D design space exploration

Experimental design point	**SEN port angle [°]**	**SEN port height [mm]**	**SEN well depth [mm]**
2.0_linear	-20	80	1 (no well recommended)[15]

[15] A 1mm well had to be simulated due to difficulties experienced in GAMBIT when a well of 0mm is endeavoured to be created using the GAMBIT script file.

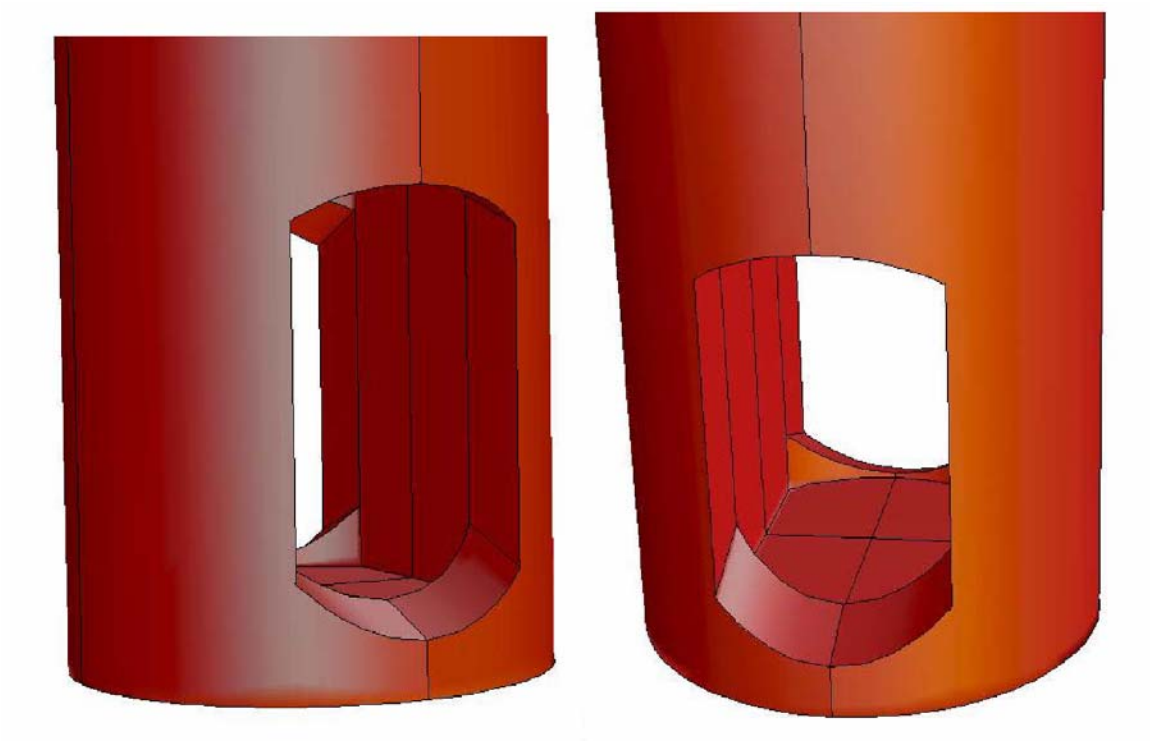

Figure 5.18: Geometry of chosen design (port angle = 20° downwards, port height = 80mm, no well)

5.6.5 Validation of chosen design with 40%-scaled water model

Using the modular SEN insert design, the 40%-scaled physical optimum Aluminium SEN design (port angle = 20° downwards, port height = 80mm (full-scale), no well) could easily be manufactured for water model testing.

If the CFD model compares favourably with the water model results of the optimum SEN, it will prove that the CFD model can be trusted for further optimisation work. This validation will simultaneously double as verification for the extension of the momentum-only CFD model to real plant circumstances, as well as proving that satisfying Fr-similarity is indeed sufficient for scaled water modelling testing.

The CFD results (depicted in Figures 5.19 – 5.20) reflect the plant circumstances (full scale), where liquid steel is used as the fluid.

The validation for the optimum SEN is performed at the wider width, 1250mm, as the wider CFD models tend to be less stable than the narrower models. The validation is also performed for three different submergence depths, namely 80mm, 150mm and 200mm. The CFD results for the 200mm submergence is shown below, and that of 80mm and 150mm are shown in Appendix Q.

The CFD results of the optimum SEN (in Figures 5.19, 5.20 and Appendix Q) surprisingly correspond closely to the water model tests, which satisfy Fr-similarity.

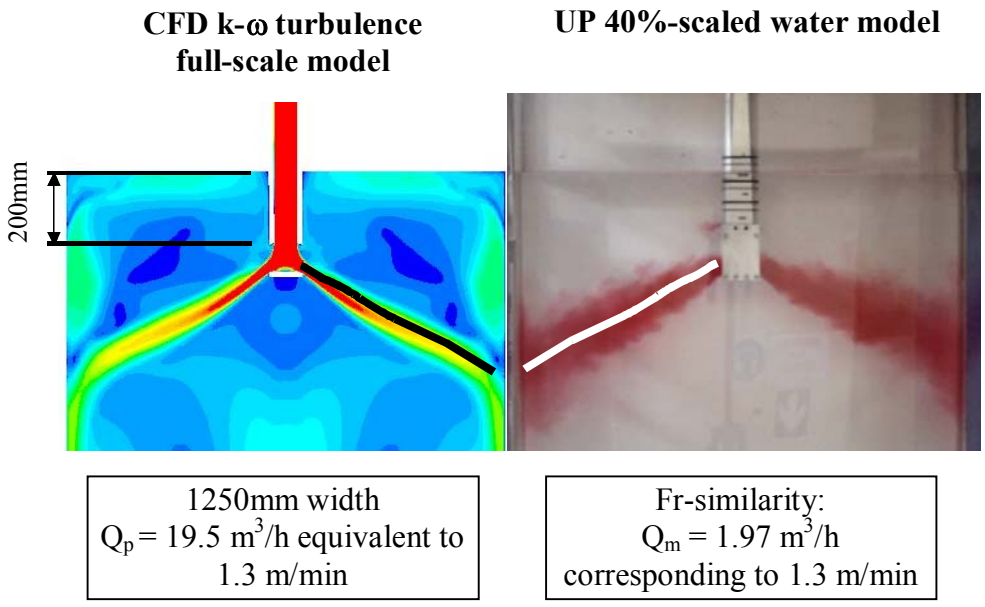

Figure 5.19: Validation of optimum SEN design at mould width 1250mm and 200mm submergence depth, using contours of velocity (scale 0 – 1 m/s)

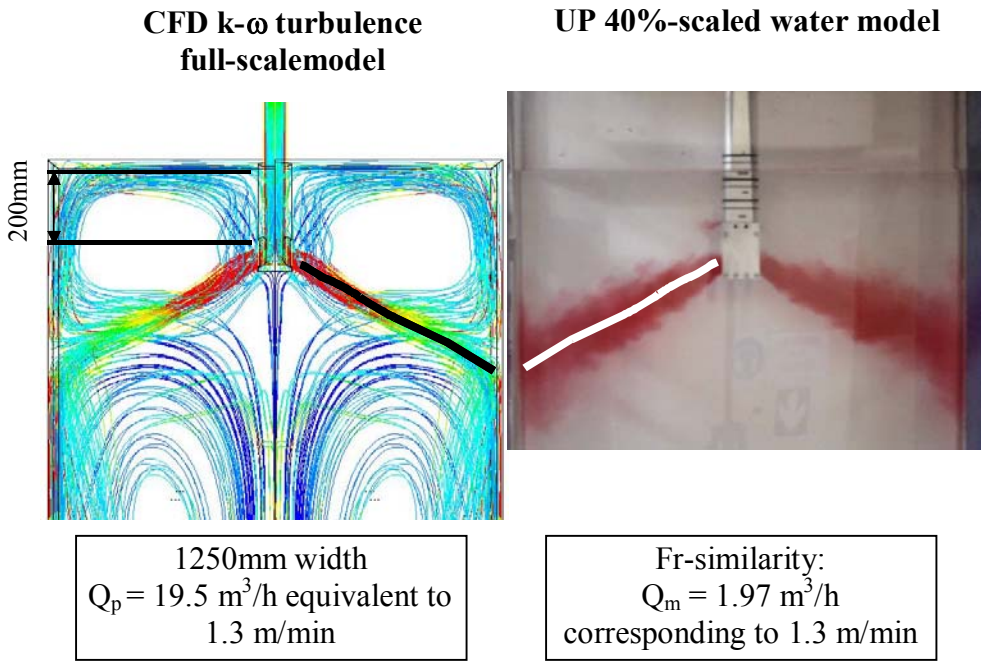

Figure 5.20: Validation of optimum SEN design at mould width 1250mm and 200mm submergence depth, using path lines coloured by velocity magnitude (scale 0 – 1 m/s)

The optimum design of the 3D design space exploration is thus validated and can confidently be recommended for manufacture for a first plant trial.

5.6.6 CFD comparison between chosen design and base case model

In order to show the potential of mathematical optimisation, the improved SEN design (from the 3D exploration study) is compared to the base case SEN design. Figure 5.21 compares the maximum TKE on the meniscus (top view) of the base case and that of the chosen design. Operational parameter values and design variable values are tabulated in Table 5.8.

Table 5.8: Values: comparison between base case and chosen design from 3D exploration study

Description	**Base case SEN design**	**Improved / Chosen design from 3D exploration study**
Experiment number	1.0	2.0_linear
SEN port angle (º)	15º	- 20º
SEN port height (mm)	70mm	80mm
SEN well depth	0mm (1mm)	0mm (1mm)
Submergence depth (mm)	200mm	200mm
Mould width (mm)	1060mm	1060mm
Mould thickness (mm)	200mm	200mm
Casting speed (m/min)	1.3 m/min	1.3 m/min

Using the same TKE range (0 – 0.002 m^2/s^2) for both SEN designs, one can clearly graphically identify the best design when measured against the objective function (minimising the maximum TKE on the meniscus).

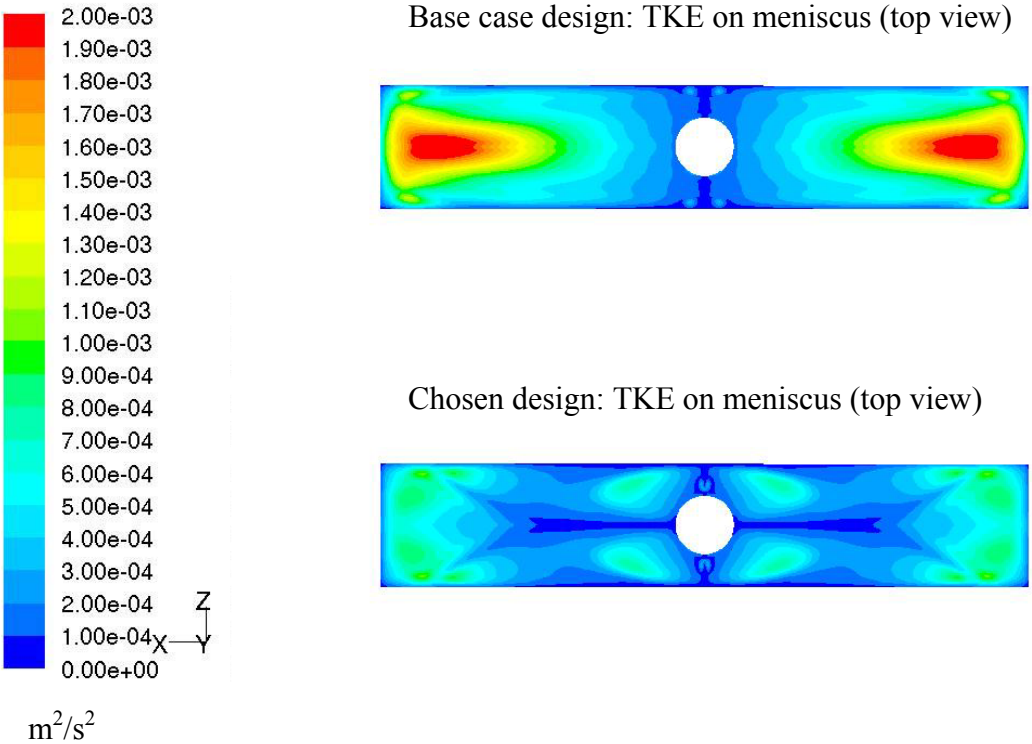

Figure 5.21: Comparison between TKE on the meniscus of the base case and chosen design from 3D exploration study for casting conditions indicated in Table 5.8

This comparison of the design space exploration optimum with the initial design (base case) concludes this chapter, which focused on mathematical optimisation of the continuous caster SEN using CFD simulations. Chapter 6 (Conclusion and Future Work) that follows, shall conclude the dissertation in its entirety.